Stuber, G.L. “Modulation Methods”
Mobile Communications Handbook
Ed. Suthan S. Suthersan
Boca Raton: CRC Press LLC, 1999

Modulation Methods

Gordon L. Stuber
Georgia Institute of Technology

16.1 Introduction

Modulation is the process where the message information is added to the radio carrier. Most first generation cellular systems such as the advanced mobile telephone system (AMPS) use analog **frequency modulation** (**FM**), because analog technology was very mature when these systems were first introduced. Digital modulation schemes, however, are the obvious choice for future wireless systems, especially if data services such as wireless multimedia are to be supported. Digital modulation can also improve spectral efficiency, because digital signals are more robust against channel impairments. Spectral efficiency is a key attribute of wireless systems that must operate in a crowded radio frequency spectrum.

To achieve high spectral efficiency, modulation schemes must be selected that have a high **bandwidth efficiency** as measured in units of bits per second per Hertz of bandwidth. Many wireless communication systems, such as cellular telephones, operate on the principle of frequency reuse, where the carrier frequencies are reused at geographically separated locations. The link quality in these systems is limited by cochannel interference. Hence, modulation schemes must be identified that are both bandwidth efficient and capable of tolerating high levels of cochannel interference. More specifically, digital modulation techniques are chosen for wireless systems that satisfy the following properties.

Compact Power Density Spectrum: To minimize the effect of adjacent channel interference, it is desirable that the power radiated into the adjacent channel be 60–80 dB below that in the desired channel. Hence, modulation techniques with a narrow main lobe and fast rolloff of sidelobes are desirable.

Good Bit-Error-Rate Performance: A low-bit-error probability should be achieved in the presence of cochannel interference, adjacent channel interference, thermal noise, and other channel impairments, such as fading and intersymbol interference.

Envelope Properties: Portable and mobile applications typically employ nonlinear (class C) power amplifiers to minimize battery drain. Nonlinear amplification may degrade the bit-error-rate performance of modulation schemes that transmit information in the amplitude of the carrier. Also, spectral shaping is usually performed prior to up-conversion and nonlinear amplification. To prevent the regrowth of spectral sidelobes during nonlinear amplification, the input signal must have a relatively constant envelope.

A variety of digital modulation techniques are currently being used in wireless communication systems. Two of the more widely used digital modulation techniques for cellular mobile radio are $\pi/4$ phase-shifted quadrature **phase shift keying** ($\pi/4$-QPSK) and **Gaussian minimum shift keying** (**GMSK**). The former is used in the North American IS-54 digital cellular system and Japanese Personal Digital Cellular (PDC), whereas the latter is used in the global system for mobile communications (GSM system). This chapter provides a discussion of these and other modulation techniques that are employed in wireless communication systems.

16.2 Basic Description of Modulated Signals

With any modulation technique, the bandpass signal can be expressed in the form

$$s(t) = \mathrm{Re}\left\{v(t)e^{j2\pi f_c t}\right\} \tag{16.1}$$

where $v(t)$ is the complex envelope, f_c is the carrier frequency, and Re$\{z\}$ denotes the real part of z. For digital modulation schemes $v(t)$ has the general form

$$v(t) = A\sum_k b\left(t - kT, \boldsymbol{x}_k\right)\psi \tag{16.2}$$

where A is the amplitude of the carrier $\boldsymbol{x}_k = (x_k, x_{k-1}, \ldots, x_{k-K})$ is the data sequence, T is the symbol or baud duration, and $b(t, \boldsymbol{x}_i)$ is an equivalent shaping function usually of duration T. The precise form of $b(t, \boldsymbol{x}_i)$ and the memory length K depends on the type of modulation that is employed. Several examples are provided in this chapter where information is transmitted in the amplitude, phase, or frequency of the bandpass signal.

The **power spectral density** of the bandpass signal $S_{ss}(f)$ is related to the power spectral density of the complex envelope $S_{vv}(f)$ by

$$S_{ss}(f) = \frac{1}{2}\left[S_{vv}\left(f - f_c\right) + S_{vv}\left(f + f_c\right)\right] \tag{16.3}$$

The power density spectrum of the complex envelope for a digital modulation scheme has the general form

$$S_{vv}(f) = \frac{A^2}{T}\sum_m S_{b,m}(f)e^{-j2\pi fmT} \tag{16.4}$$

where

$$S_{b,m}(f) = \frac{1}{2}E\left[B\left(f, \boldsymbol{x}_m\right)B^*\left(f, \boldsymbol{x}_0\right)\right] \tag{16.5}$$

$B(f, \boldsymbol{x}_m)$ is the Fourier transform of $b(t, \boldsymbol{x}_m)$, and $E[\cdot]$ denotes the expectation operator. Usually symmetric signal sets are chosen so that the complex envelope has zero mean, i.e., $E[b(t, \boldsymbol{x}_0)] = 0$.

This implies that the power density spectrum has no discrete components. If, in addition, $\boldsymbol{x}_m$ and $\boldsymbol{x}_0$ are independent for $|m| > K$, then

$$S_{vv}(f) = \frac{A^2}{T} \sum_{|m|<K} S_{b,m}(f) e^{-j2\pi f m T} \tag{16.6}$$

16.3 Analog Frequency Modulation

With analog frequency modulation the complex envelope is

$$v(t) = A \exp\left[j2\pi k_f \int_0^t m(\tau)\, \mathrm{d}\tau \right] \tag{16.7}$$

where $m(t)$ is the modulating waveform and k_f in Hz/v is the frequency sensitivity of the FM modulator. The bandpass signal is

$$s(t) = A \cos\left[2\pi f_c t + 2\pi k_f \int_0^t m(t)\, \mathrm{d}t \right] . \tag{16.8}$$

The instantaneous frequency of the carrier $f_i(t) = f_c + k_f m(t)$ varies linearly with the waveform $m(t)$, hence, the name frequency modulation. Notice that FM has a constant envelope making it suitable for nonlinear amplification. However, the complex envelope is a nonlinear function of the modulating waveform $m(t)$ and, therefore, the spectral characteristics of $v(t)$ cannot be obtained directly from the spectral characteristics of $m(t)$.

With the sinusoidal modulating waveform $m(t) = A_m \cos(2\pi f_m t)$ the instantaneous carrier frequency is

$$f_i(t) = f_c + \Delta_f \cos(2\pi f_m t) \tag{16.9}$$

where $\Delta_f = k_f A_m$ is the peak frequency deviation. The complex envelope becomes

$$\begin{aligned} v(t) &= \exp\left[2\pi \int_0^t f_i(t)\, \mathrm{d}t \right] \\ &= \exp\left[2\pi f_c t + \beta \sin(2\pi f_m t) \right] \end{aligned} \tag{16.10}$$

where $\beta = \Delta_f / f_m$ is called the modulation index. The bandwidth of $v(t)$ depends on the value of β. If $\beta < 1$, then narrowband FM is generated, where the spectral widths of $v(t)$ and $m(t)$ are about the same, i.e., $2f_m$. If $\beta \gg 1$, then wideband FM is generated, where the spectral occupancy of $v(t)$ is slightly greater than $2\Delta_f$. In general, the approximate bandwidth of an FM signal is

$$W \approx 2\Delta_f + 2f_m = 2\Delta_f \left(1 + \frac{1}{\beta} \right) \tag{16.11}$$

which is a relation known as Carson's rule. Unfortunately, typical analog cellular radio systems use a modulation index in the range $1 \lessapprox \beta \lessapprox 3$ where Carson's rule is not accurate. Furthermore, the message waveform $m(t)$ is not a pure sinusoid so that Carson's rule does not directly apply.

In analog cellular systems the waveform $m(t)$ is obtained by first companding the speech waveform and then hard limiting the resulting signal. The purpose of the limiter is to control the peak frequency deviation Δ_f. The limiter introduces high-frequency components that must be removed with a low-pass filter prior to modulation. To estimate the bandwidth occupancy, we first determine the ratio of the frequency deviation Δ_f corresponding to the maximum amplitude of $m(t)$, and the highest frequency component B that is present in $m(t)$. These two conditions are the most extreme cases, and the resulting ratio, $D = \Delta_f / B$, is called the *deviation ratio*. Then replace β by D and f_m by B in Carson's rule, giving

$$W \approx 2\Delta_f + 2B = 2\Delta_f \left(1 + \frac{1}{D}\right) \tag{16.12}$$

This approximation will overestimate the bandwidth requirements. A more accurate estimate of the bandwidth requirements must be obtained from simulation or measurements.

16.4 Phase Shift Keying (PSK) and $\pi/4$-QPSK

With **phase shift keying** (PSK), the equivalent shaping function in Eq. (16.2) has the form

$$b\left(t, \boldsymbol{x}_k\right) = \psi_T(t) \exp\left[j \frac{\pi}{M} x_k h_s(t)\right], \psi \qquad \boldsymbol{x}_k = x_k \tag{16.13}$$

where $h_s(t)$ is a phase shaping pulse, $\psi_T(t)$ an amplitude shaping pulse, and M the size of the modulation alphabet. Notice that the phase varies linearly with the symbol sequence $\{x_k\}$, hence the name phase shift keying. For a modulation alphabet size of M, $x_k \in \{\pm 1, \pm 3, \ldots, \pm(M-1)\}$. Each symbol x_k is mapped onto $\log_2 M$ source bits. A QPSK signal is obtained by using $M = 4$, resulting in a transmission rate of 2 b/symbol.

Usually, the phase shaping pulse is chosen to be the rectangular pulse $h_s(t) = u_T(t) \triangleq u(t) - u(t-T)$, where $u(t)$ is the unit step function. The amplitude shaping pulse is very often chosen to be a square root raised cosine pulse, where the Fourier transform of $\psi_T(t)$ is

$$\Psi_T(f) = \begin{cases} \sqrt{T}\psi & 0 \le |f| \le (1-\beta)/2T \\ \sqrt{\dfrac{T}{2}\left[1 - \sin\dfrac{\pi T}{\beta}\left(f - \dfrac{1}{2T}\right)\right]} & (1-\beta)/2T \le |f| \le (1+\beta)/2T \end{cases} \tag{16.14}$$

The receiver implements the same filter $\Psi_R(f) = \Psi_T(f)$ so that the overall pulse has the raised cosine spectrum $\Psi(f) = \Psi_R(f)\Psi_T(f) = |\Psi_T(f)|^2$. If the channel is affected by flat fading and additive white Gaussian noise, then this partitioning of the filtering operations between the transmitter and receiver will optimize the signal to noise ratio at the output of the receiver filter at the sampling instants. The rolloff factor β usually lies between 0 and 1 and defines the **excess bandwidth** $100\beta\%$. Using a smaller β results in a more compact power density spectrum, but the link performance becomes more sensitive to errors in the symbol timing. The IS-54 system uses $\beta = 0.35$, while PDC uses $\beta = 0.5$.

The time domain pulse corresponding to Eq. (16.14) can be obtained by taking the inverse Fourier transform, resulting in

$$\psi_T(t) = 4\beta \frac{\cos\left[(1+\beta)\pi t/T\right] + \sin\left[(1-\beta)\pi t/T\right](4\beta t/T)^{-1}}{\pi\sqrt{T}\left[1 - 16\beta^2 t^2/T^2\right]} \tag{16.15}$$

A typical square root raised cosine pulse with a rolloff factor of $\beta = 0.5$ is shown in Fig. 16.1. Strictly speaking the pulse $\psi_T(t)$ is noncausal, but in practice a truncated time domain pulse is used. For example, in Fig. 16.1 the pulse is truncated to $6T$ and time shifted by $3T$ to yield a causal pulse.

Unlike conventional QPSK that has four possible transmitted phases, $\pi/4$-QPSK has eight possible transmitted phases. Let $\theta(n)$ be the transmitted carrier phase for the nth epoch, and let $\Delta\theta(n) =$

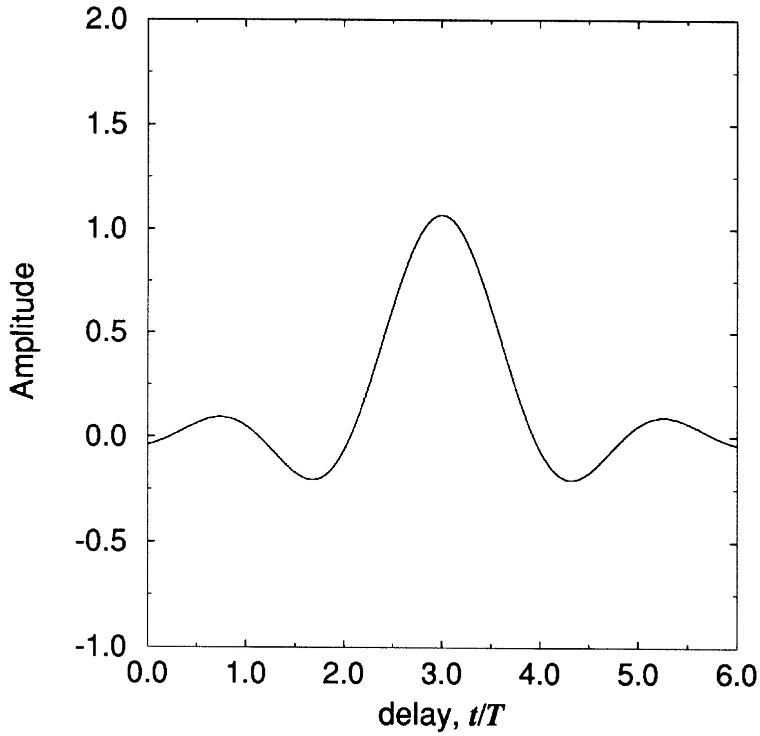

FIGURE 16.1: Square root raised cosine pulse with rolloff factor $\beta = 0.5$.

$\theta(n) - \theta(n-1)$ be the differential carrier phase between epochs n and $n-1$. With $\pi/4$-QPSK, the transmission rate is 2 b/symbol and the differential phase is related to the symbol sequence $\{x_n\}$ through the mapping

$$\Delta\theta(n) = \begin{cases} -3\pi/4, & x_n = -3 \\ -\pi/4, & x_n = -1 \\ \pi/4, & x_n = +1 \\ 3\pi/4, & x_n = +3 \end{cases} \tag{16.16}$$

Since the symbol sequence $\{x_n\}$ is random, the mapping in Eq. (16.16) is arbitrary, except that the phase differences must be $\pm\pi/4$ and $\pm 3\pi/4$. The phase difference with the given mapping can be written in the convenient algebraic form

$$\Delta\theta(n) = x_n \frac{\pi}{4} \tag{16.17}$$

which allows us to write the equivalent shaping function of the $\pi/4$-QPSK signal as

$$\begin{aligned} b\left(t, \underline{\boldsymbol{x}}_k\right) &= \psi(t)\exp\left\{j\left[\theta(k-1) + x_k\frac{\pi}{4}\right]\right\} \\ &= \psi_T(t)\exp\left[j\frac{\pi}{4}\left(\sum_{n=-\infty}^{k-1} x_n + x_k\right)\right] \end{aligned} \tag{16.18}$$

The summation in the exponent represents the accumulated carrier phase, whereas the last term is the phase change due to the kth symbol. Observe that the phase shaping function is the rectangular pulse $u_T(t)$. The amplitude shaping function $\psi_T(t)$ is usually the square root raised cosine pulse in Eq. (16.15).

The phase states of QPSK and $\pi/4$-QPSK signals can be summarized by the signal space diagram in Fig. 16.2 that shows the phase states and allowable transitions between the phase states. However, it does not describe the actual phase trajectories. A typical diagram showing phase trajectories with square root raised cosine pulse shaping is shown in Fig. 16.3. Note that the phase trajectories do not pass through the origin. This reduces the envelope fluctuations of the signal making it less susceptible to amplifier nonlinearities and reduces the dynamic range required of the power amplifier.

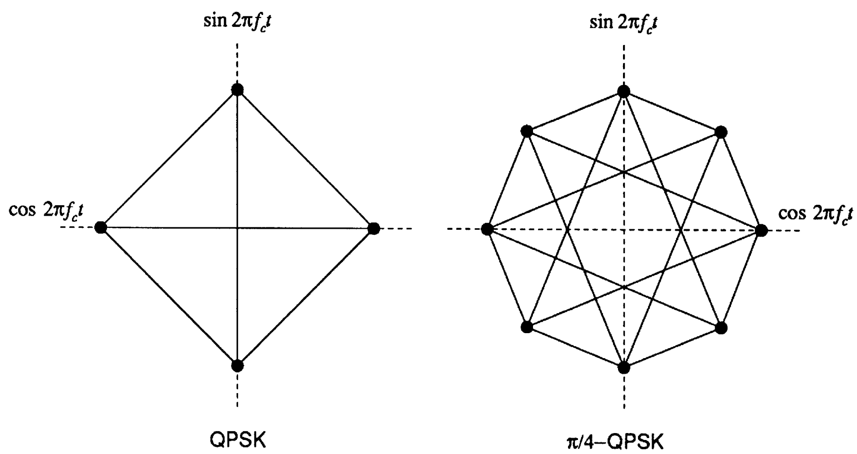

FIGURE 16.2: Signal-space constellations for QPSK and $\pi/4$-DQPSK.

The power density spectrum of QPSK and $\pi/4$-QPSK depends on both the amplitude and phase shaping pulses. For the rectangular phase shaping pulse $h_s(t) = u_T(t)$, the power density spectrum of the complex envelope is

$$S_{vv}(f) = \frac{A^2}{T} |\Psi_T(f)|^2 \tag{16.19}$$

With square root raised cosine pulse shaping, $\Psi_T(f)$ has the form defined in Eq. (16.14). The power density spectrum of a pulse $\tilde{\psi}_T(t)$ that is obtained by truncating $\psi_T(t)$ to length τ can be obtained by writing $\tilde{\psi}_T(t) = \psi_T(t)\text{rect}(t/\tau)$. Then $\tilde{\Psi}_T(f) = \Psi_T(f) * \tau\text{sinc}(f\tau)$, where $*$ denotes the operation of convolution, and the power density spectrum is again obtained by applying Eq. (16.19). Truncation of the pulse will regenerate some side lobes, thus causing adjacent channel interference. Figure 16.4 illustrates the power density spectrum of a truncated square root raised cosine pulse for various truncation lengths τ.

16.5 Continuous Phase Modulation (CPM) and MSK

Continuous phase modulation (**CPM**) refers to a broad class of frequency modulation techniques where the carrier phase varies in a continuous manner. A comprehensive treatment of CPM is provided in [1]. CPM schemes are attractive because they have constant envelope and excellent

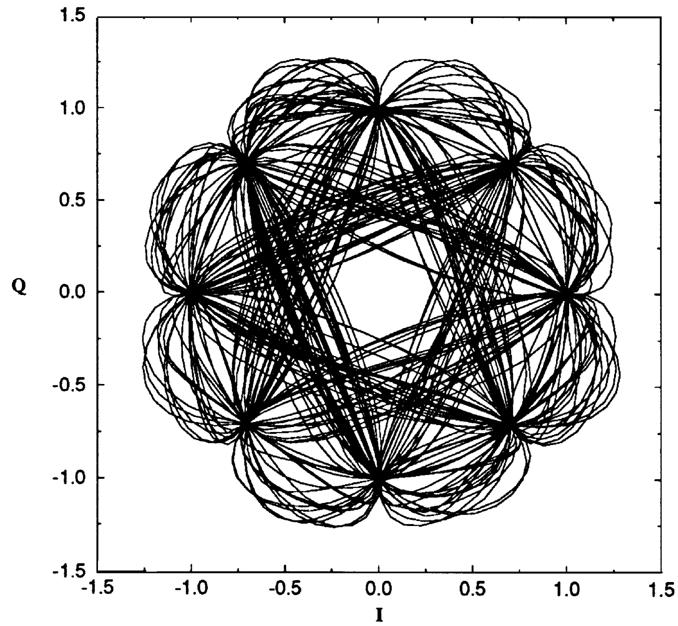

FIGURE 16.3: Phase diagram of $\pi/4$-QPSK with square root raised cosine pulse; $\beta = 0.5$.

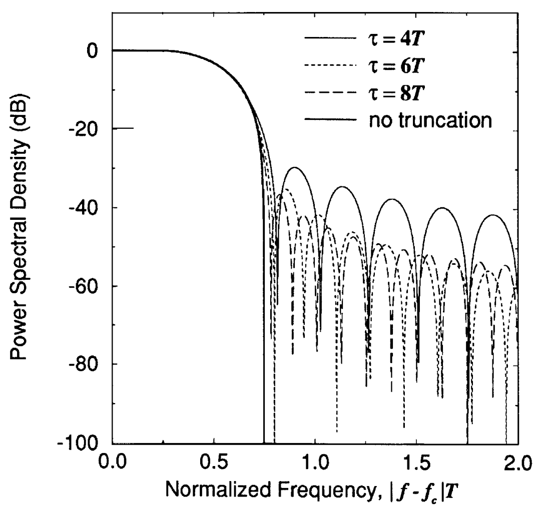

FIGURE 16.4: Power density spectrum of truncated square root raised cosine pulse with various truncation lengths; $\beta = 0.5$.

spectral characteristics. The complex envelope of any CPM signal is

$$v(t) = A \exp\left[j2\pi k_f \int_{-\infty}^{t} \sum_n x_n h_s(\tau - nT)\, \mathrm{d}\tau \right] \tag{16.20}$$

The instantaneous frequency deviation from the carrier is

$$f_{\text{dev}}(t) = k_f \sum_n x_n h_s(t - nT) \tag{16.21}$$

where k_f is the peak frequency deviation. If the frequency shaping pulse $h_s(t)$ has duration T, then the equivalent shaping function in Eq. (16.2) has the form

$$b\,(t, \boldsymbol{x}_k) = \exp\left\{ j \left[\beta(T) \sum_{n=-\infty}^{k-1} x_n + x_k \beta(t) \right] \right\} u_T(t) \tag{16.22}$$

where

$$\beta(t) = \begin{cases} 0, & t < 0 \\ \dfrac{\pi h}{\int_0^T h_s(\tau)\,\mathrm{d}\tau} \displaystyle\int_0^t h_s(\tau)\,\mathrm{d}\tau, & 0 \le t \le T \\ \pi h, & t \ge T \end{cases} \tag{16.23}$$

is the phase shaping pulse, and $h = \beta(T)/\pi$ is called the modulation index.

Minimum shift keying (**MSK**) is a special form of binary CPM ($x_k \in \{-1, +1\}$) that is defined by a rectangular frequency shaping pulse $h_s(t) = u_T(t)$, and a modulation index $h = 1/2$ so that

$$\beta(t) = \begin{cases} 0, & t < 0 \\ \pi t/2T, & 0 \le t \le T \\ \pi/2, & t \ge T \end{cases} \tag{16.24}$$

Therefore, the complex envelope is

$$v(t) = A \exp\left(j \frac{\pi}{2} \sum_{n=-\infty}^{k-1} x_n + \frac{\pi}{2} x_k \frac{t - kT}{T} \right) \tag{16.25}$$

A MSK signal can be described by the phase trellis diagram shown in Fig. 16.5 which plots the time behavior of the phase

$$\theta(t) = \frac{\pi}{2} \sum_{n=-\infty}^{k-1} x_n + \frac{\pi}{2} x_k \frac{t - kT}{T} \tag{16.26}$$

The MSK bandpass signal is

$$\begin{aligned} s(t) &= A\cos\left(2\pi f_c t + \frac{\pi}{2} \sum_{n=-\infty}^{k-1} x_n + \frac{\pi}{2} x_k \frac{t - kT}{T} \right) \\ &= A\cos\left[2\pi \left(f_c + \frac{x_k}{4T} \right) t - \frac{k\pi}{2} x_k + \frac{\pi}{2} \sum_{n=-\infty}^{k-1} x_n \right] \quad kT \le t \le (k+1)T \end{aligned} \tag{16.27}$$

From Eq. (16.27) we observe that the MSK signal has one of two possible frequencies $f_L = f_c - 1/4T$ or $f_U = f_c + 1/4T$ during each symbol interval. The difference between these frequencies is $f_U - f_L = 1/2T$. This is the minimum frequency difference between two sinusoids of duration

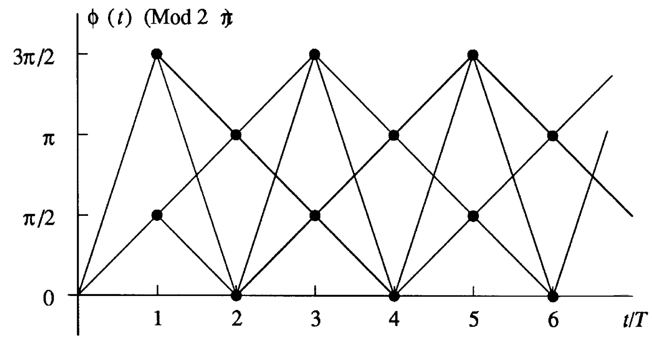

FIGURE 16.5: Phase-trellis diagram for MSK.

T that will ensure orthogonality with coherent demodulation [7], hence, the name minimum shift keying. By applying various trigonometric identities to Eq. (16.27) we can write

$$
\begin{aligned}
s(t) &= A\left[x_k^I \psi(t-k2T)\cos(2\pi f_c t) - x_k^Q \psi(t-k2T-T)\sin(2\pi f_c t)\right], \\
&\qquad\qquad kT \le t \le (k+1)T
\end{aligned}
\tag{16.28}
$$

where

$$
\begin{aligned}
x_k^I &= -x_{k-1}^Q x_{2k-1} \\
x_k^Q &= x_k^I x_{2k} \\
\psi(t) &= \cos\left(\frac{\pi t}{2T}\right), \qquad -T \le t \le T
\end{aligned}
$$

Note that the x_k^I and x_k^Q are independent binary symbols that take on elements from the set $\{-1, +1\}$, and the half-sinusoid amplitude shaping pulse $\psi(t)$ has duration $2T$ and $\psi(t-T) = \sin(\pi t/2T)$, $0 \le t \le 2T$. Therefore, MSK is equivalent to offset quadrature amplitude shift keying (OQASK) with a half-sinusoid amplitude shaping pulse.

To obtain the power density spectrum of MSK, we observe from Eq. (16.28) that the equivalent shaping function of MSK has the form

$$
b(t, \boldsymbol{x}_k) = x_k^I \psi(t) + j x_k^Q \psi(t-T) \tag{16.29}
$$

The Fourier transform of Eq. (16.29) is

$$
B(f, \boldsymbol{x}_k) = \left(x_k^I + j x_k^Q e^{-j2\pi f T}\right)\Psi(f) \tag{16.30}
$$

Since the symbols x_k^I and x_k^Q are independent and zero mean, it follows from Eqs. (16.5) and (16.6) that

$$
S_{vv}(f) = \frac{A^2|\Psi(f)|^2}{2T} \tag{16.31}
$$

Therefore, the power density spectrum of MSK is determined solely by the Fourier transform of the half-sinusoid amplitude shaping pulse $\psi(t)$, resulting in

$$
S_{vv}(f) = \frac{16A^2T}{\pi^2}\left[\frac{\cos 2\pi f T}{1-16f^2T^2}\right]^2 \tag{16.32}
$$

The power spectral density of MSK is plotted in Fig. 16.8. Observe that an MSK signal has fairly large sidelobes compared to $\pi/4$-QPSK with a truncated square root raised cosine pulse (c.f., Fig. 16.4).

16.6 Gaussian Minimum Shift Keying

MSK signals have all of the desirable attributes for mobile radio, except for a compact power density spectrum. This can be alleviated by filtering the modulating signal $x(t) = \Sigma_n x_n u_T(t - nT)$ with a low-pass filter prior to frequency modulation, as shown in Fig. 16.6. Such filtering removes the higher frequency components in $x(t)$ and, therefore, yields a more compact spectrum. The low-pass filter is chosen to have 1) narrow bandwidth and a sharp transition band, 2) low-overshoot impulse response, and 3) preservation of the output pulse area to ensure a phase shift of $\pi/2$.

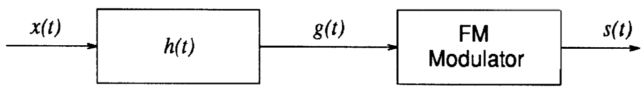

FIGURE 16.6: Premodulation filtered MSK.

GMSK uses a low-pass filter with the following transfer function:

$$H(f) = A \exp\left\{-\left(\frac{f}{B}\right)^2 \frac{\ln 2}{2}\right\} \tag{16.33}$$

where B is the 3-dB bandwidth of the filter and A a constant. It is apparent that $H(f)$ is bell shaped about $f = 0$, hence the name Gaussian MSK. A rectangular pulse $\mathrm{rect}(t/T) = u_T(t + T/2)$ transmitted through this filter yields the frequency shaping pulse

$$h_s(t) = A\sqrt{\frac{2\pi}{\ln 2}}(BT) \int_{t/T-1/2}^{t/T+1/2} \exp\left\{-\frac{2\pi^2(BT)^2x^2}{\ln 2}\right\} \mathrm{d}x \tag{16.34}$$

The phase change over the time interval from $-T/2 \le t \le T/2$ is

$$\theta\left(\frac{T}{2}\right) - \theta\left(\frac{-T}{2}\right) = x_0\beta_0(T) + \sum_{\substack{n=-\infty \\ n\neq 0}}^{\infty} x_n\beta_n(T) \tag{16.35}$$

where

$$\beta_n(T) = \frac{\pi h}{\int_{-\infty}^{\infty} h_s(\nu)\,\mathrm{d}\nu} \int_{-T/2-nT}^{T/2-nT} h_s(\nu)\,\mathrm{d}\nu \tag{16.36}$$

The first term in Eq. (16.35) is the desired term, and the second term is the intersymbol interference (ISI) introduced by the premodulation filter. Once again, with GMSK $h = 1/2$ so that a total phase shift of $\pi/2$ is maintained.

Notice that the pulse $h_s(t)$ is noncausal so that a truncated pulse must be used in practice. Figure 16.7 plots a GMSK frequency shaping pulse that is truncated to $\tau = 5T$ and time shifted by $2.5T$, for various normalized filter bandwidths BT. Notice that the frequency shaping pulse has a duration greater than T so that ISI is introduced. As BT decreases, the induced ISI is increased.

Thus, whereas a smaller value of BT results in a more compact power density spectrum, the induced ISI will degrade the bit-error-rate performance. Hence, there is a tradeoff in the choice of BT. Some studies have indicated that $BT = 0.25$ is a good choice for cellular radio systems [6].

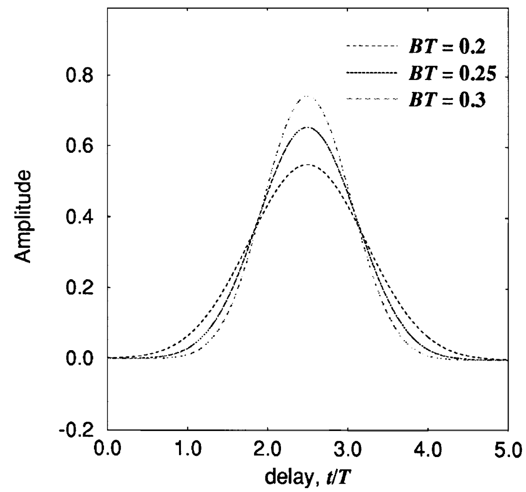

FIGURE 16.7: GMSK frequency shaping pulse for various normalized filter bandwidths BT.

The power density spectrum of GMSK is quite difficult to obtain, but can be computed by using published methods [3]. Figure 16.8 plots the power density spectrum for $BT = 0.2$, 0.25, and 0.3, obtained from Wesolowski, [8]. Observe that the spectral sidelobes are greatly reduced by the Gaussian low-pass filter.

16.7 Orthogonal Frequency Division Multiplexing (OFDM)

Orthogonal frequency division multiplexing (**OFDM**) is a modulation technique that has been recently suggested for use in cellular radio [2], digital audio broadcasting [4], and digital video broadcasting. The basic idea of OFDM is to transmit blocks of symbols in parallel by employing a (large) number of orthogonal subcarriers. With block transmission, N serial source symbols each with period T_s are converted into a block of N parallel modulated symbols each with period $T = NT_s$. The block length N is chosen so that $NT_s \gg \sigma_\tau$, where σ_τ is the rms delay spread of the channel. Since the symbol rate on each subcarrier is much less than the serial source rate, the effects of delay spread are greatly reduced. This has practical advantages because it may reduce or even eliminate the need for equalization. Although the block length N is chosen so that $NT_s \gg \sigma_\tau$, the channel dispersion will still cause consecutive blocks to overlap. This results in some residual ISI that will degrade the performance. This residual ISI can be eliminated at the expense of channel capacity by using guard intervals between the blocks that are at least as long as the effective channel impulse response.

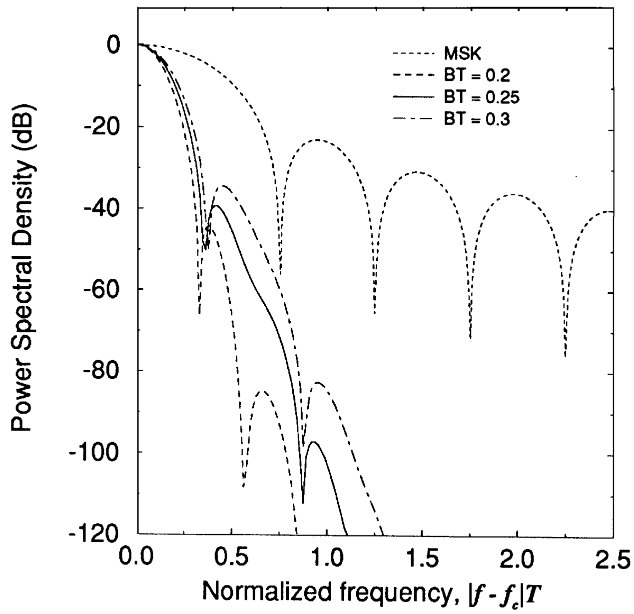

FIGURE 16.8: Power density spectrum of MSK and GMSK.

The complex envelope of an OFDM signal is described by

$$v(t) = A \sum_{k} \sum_{n=0}^{N-1} x_{k,n} \phi_n(t - kT) \psi \tag{16.37}$$

where

$$\phi_n(t) = \exp\left\{ j \frac{2\pi \left(n - \frac{N-1}{2} \right) t}{T} \right\} U_T(t), \psi \qquad n = 0, 1, \ldots, N-1 \tag{16.38}$$

are orthogonal waveforms and $U_T(t)$ is a rectangular shaping function. The frequency separation of the subcarriers, $1/T$, ensures that the subcarriers are orthogonal and phase continuity is maintained from one symbol to the next, but is twice the minimum required for orthogonality with coherent detection. At epoch k, N-data symbols are transmitted by using the N distinct pulses. The data symbols $x_{k,n}$ are often chosen from an M-ary **quadrature amplitude modulation** (M-QAM) constellation, where $x_{k,n} = x^I_{k,n} + j x^Q_{k,n}$ with $x^I_{k,n}, x^Q_{k,n} \in \{\pm 1, \pm 3, \ldots, \pm(N-1)\}$ and $N = \sqrt{M}$.

A key advantage of using OFDM is that the modulation can be achieved in the discrete domain by using either an inverse discrete Fourier transform (IDFT) or the more computationally efficient inverse fast Fourier transform (IFFT). Considering the data block at epoch $k = 0$ and ignoring the frequency offset $\exp\{-j[2\pi(N-1)t/2T]\}$, the complex low-pass OFDM signal has the form

$$v(t) = \sum_{n=0}^{N-1} x_{0,n} \exp\left\{ \frac{j 2\pi n t}{N T_s} \right\}, \psi \qquad 0 \le t \le T\psi \tag{16.39}$$

If this signal is sampled at epochs $t = kT_s$, then

$$v^k = v\left(kT_s\right) = \sum_{n=0}^{N-1} x_{0,n} \exp\left\{\frac{j2\pi nk}{N}\right\}, \qquad k = 0, 1, \ldots, N-1 \tag{16.40}$$

Observe that the sampled OFDM signal has duration N and the samples $v^0, v^1, \ldots, v^{N-1}$ are just the IDFT of the data block $x_{0,0}, x_{0,1}, \ldots, x_{0,N-1}$. A block diagram of an OFDM transmitter is shown in Fig. 16.9.

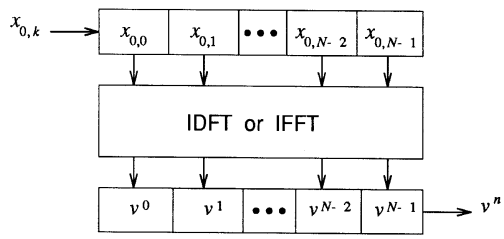

FIGURE 16.9: Block diagram of OFDM transmitter using IDFT or IFFT.

The power spectral density of an OFDM signal can be obtained by treating OFDM as independent modulation on subcarriers that are separated in frequency by $1/T$. Because the subcarriers are only separated by $1/T$, significant spectral overlap results. Because the subcarriers are orthogonal, however, the overlap improves the spectral efficiency of the scheme. For a signal constellation with zero mean and the waveforms in Eq. (16.38), the power density spectrum of the complex envelope is

$$S_{vv}(f) = \frac{A^2}{T}\sigma_x^2 \sum_{n=0}^{N-1} \left|\operatorname{sinc}\left[fT - \left(n - \frac{N-1}{2}\right)\right]\right|^2 \tag{16.41}$$

where $\sigma_x^2 = \frac{1}{2}E[|x_{k,n}|^2]$ is the variance of the signal constellation. For example, the complex envelope power spectrum of OFDM with $N = 32$ subcarriers is shown in Fig. 16.10.

16.8 Conclusions

A variety of modulation schemes are employed in wireless communication systems. Wireless modulation schemes must have a compact power density spectrum, while at the same time providing a good bit-error-rate performance in the presence of channel impairments such as cochannel interference and fading. The most popular digital modulation techniques employed in wireless systems are GMSK in the European GSM system, $\pi/4$-QPSK in the North American IS-54 and Japanese PDC systems, and OFDM in digital audio broadcasting systems.

Defining Terms

Bandwidth efficiency: Transmission efficiency of a digital modulation scheme measured in units of bits per second per Hertz of bandwidth.

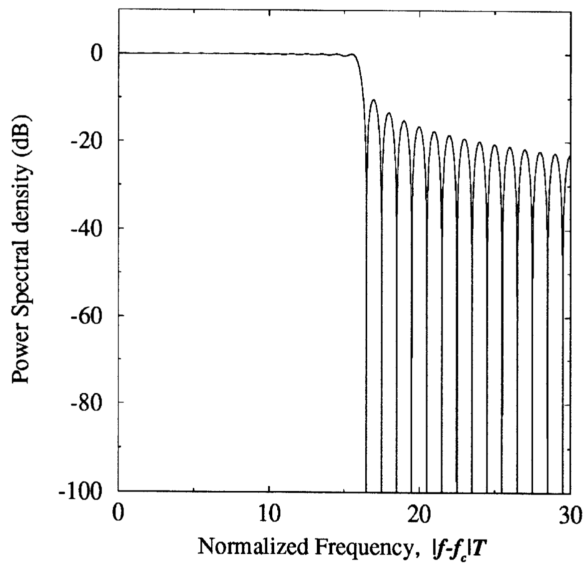

FIGURE 16.10: Power density spectrum of OFDM with $N = 32$.

Continuous phase modulation: Frequency modulation where the phase varies in a continuous manner.

Excess bandwidth: Percentage of bandwidth that is in excess of the minimum of $1/2T$ (T is the baud or symbol duration) required for data communication.

Frequency modulation: Modulation where the instantaneous frequency of the carrier varies linearly with the data signal.

Gaussian minimum shift keying: MSK where the data signal is prefiltered with a Gaussian filter prior to frequency modulation.

Minimum shift keying: A special form of continuous phase modulation having linear phase trajectories and a modulation index of $1/2$.

Orthogonal frequency division multiplexing: Modulation by using a collection of low-bit-rate orthogonal subcarriers.

Phase shift keying: Modulation where the instantaneous phase of the carrier varies linearly with the data signal.

Power spectral density: Relative power in a modulated signal as a function of frequency.

Quadrature amplitude modulation: Modulation where information is transmitted in the amplitude of the cosine and sine components of the carrier.

References

[1] Anderson, J.B., Aulin, T., and Sundberg, C.-E., *Digital Phase Modulation,* Plenum Press, New York, 1986.

[2] Birchler, M.A. and Jasper, S.C., A 64 kbps digital land mobile radio system employing M-16QAM. *Proc. 5th Nordic Sem. Dig. Mobile Radio Commun.,* 237–241, Dec. 1992.

[3] Garrison, G.J., A power spectral density analysis for digital FM, *IEEE Trans. Commun.*, COM-23, 1228–1243, Nov. 1975.
[4] Le Floch, B., Halbert-Lassalle, R., and Castelain, D., Digital sound broadcasting to mobile receivers, *IEEE Trans. Consum. Elec.*, 35, Aug. 1989.
[5] Murota, K. and Hirade, K., GMSK modulation for digital mobile radio telephony, *IEEE Trans. Commun.*, COM-29, 1044–1050, Jul. 1981.
[6] Murota, K., Kinoshita, K., and Hirade, K., Spectral efficiency of GMSK land mobile radio. *Proc. ICC'81*, 23.8.1, Jun. 1981.
[7] Proakis, J.G., *Digital Communications,* 2nd ed., McGraw-Hill, New York, 1989.
[8] Wesolowski, K., Private Communication, 1994.

Further Information

A good discussion of digital modem techniques is presented in *Advanced Digital Communications,* edited by K. Feher, Prentice-Hall, 1987.

Proceedings of various IEEE conferences such as the Vehicular Technology Conference, International Conference on Communications, and Global Telecommunications Conference, document the lastest development in the field of wireless communications each year.

Journals such as the *IEEE Transactions on Communications* and *IEEE Transactions on Vehicular Technology* report advances in wireless modulation.